

Efficient universal quantum channel simulation in IBM's cloud quantum computer

Shi-Jie Wei,^{1,*} Tao Xin,^{1,*} and Gui-Lu Long^{1,2,3,†}

¹State Key Laboratory of Low-Dimensional Quantum Physics and
Department of Physics, Tsinghua University, Beijing 100084, China

²Tsinghua National Laboratory for Information Science and Technology, Beijing 100084, P. R. China.

³Collaborative Innovation Center of Quantum Matter, Beijing 100084, China

(Dated: June 27, 2017)

The study of quantum channels is the fundamental field and promises wide range of applications, because any physical process can be represented as a quantum channel transforming an initial state into a final state. Inspired by the method performing non-unitary operator by the linear combination of unitary operations, we proposed a quantum algorithm for the simulation of universal single-qubit channel, described by a convex combination of 'quasiextreme' channels corresponding to four Kraus operators, and is scalable to arbitrary higher dimension. We demonstrate the whole algorithm experimentally using the universal IBM cloud quantum computer and study properties of different qubit quantum channels. We illustrate the quantum capacity of the general qubit quantum channels, which quantifies the amount of quantum information that can be protected. The behaviour of quantum capacity in different channels reveal which types of noise processes can support information transmission, and which types are too destructive to protect information. There is a general agreement between the theoretical predictions and the experiments, which strongly supported our method. By realizing arbitrary qubit channel, this work provides a universal way to explore various properties of quantum channel and novel prospect of quantum communication.

PACS numbers: 03.67.Ac, 03.67.Lx, 42.50.Pq, 85.25.Cp

I. INTRODUCTION

Since Feynman [1] proposed the idea of quantum computer and envisioned the possibility of efficiently simulating quantum systems, significant progress has been made in closed system quantum simulation. Quantum simulation can efficiently simulate the dynamics of diverse systems[1, 2] in condensed matter [3, 4], quantum chemistry[5], and high-energy physics[6–8], which is intractable on classical computers. Moreover, every practical quantum system is open system because of the inevitable coupling to the environment. Thus, quantum simulation of open system is an equally important and more general subject to explore. However, open quantum system simulation is still in the early stages of development and is concentrated on simulating Markovian dynamics by Lindblad master equation [9–14], which remains largely unexplored. The quantum simulation of open system promises powerful applications in a class of physical problem, such as preparing various special state [15–19], thermalizing in spin-boson systems and complex many fermion-boson systems[20, 21], studying nonequilibrium dynamics[22]. Contrary to common sense, dissipative dynamics which is not necessarily unitary can be utilized to perform universal quantum computation[23].

Given the importance of the simulation of open quantum system, efficiently performing quantum channels which represent the most general quantum dynamics pos-

sible is critical. A straightforward way suggested by the Stinespring dilation theorem [24] for the simulation of open quantum systems is to enlarge the system to include the environment, which can be regarded as a bigger closed quantum system. Then, we can perform Hamiltonian-generated unitary transformation as same as in the closed system, which means we can implement a channel as a unitary operator on an expanded Hilbert space. The evolution of the density matrix [25]

$$\rho' = \text{tr}_{env}(U(\rho \otimes \rho_{env})U^\dagger), \quad (1)$$

where ρ' is the density matrix of the final state of principal system, tr_{env} is a partial trace over environment and U is time evolution operator imposed on the total system. The disadvantage in this method is that the expanded Hilbert space dimension is at most dimension n^3 of the original system because of an environment of dimension n^2 is necessary, which make it inefficient on high dimension. In recent years, many works have been done for achieving channels in special cases [26–31], or generating arbitrary channels with significant failure probability[32]. It is worth to recall the brilliant idea of Wang *et al* which realised any qubit channel by Kraus operators with single qubit gates and controlled NOT gates [33], makes it possible to implement with current technology.

Here we present a new method which can realize universal qubit channels deterministically with controlled NOT operations. In contrast with the method suggested in [33], the approach is a total quantum algorithm without a classical random number in generator and realise four Kraus operators simultaneously. This algorithm requires two qubits maximum as ancillary system to simulate the environment by performing the controlled oper-

* These authors contributed equally to this work.

† Correspondence and requests for materials should be addressed to G.L.L.: gllong@tsinghua.edu.cn

ations on the single-qubit work system. Moreover, there are only single direction controlled operations from ancillary system to work qubit which are not dependent on the state of the single-qubit work system, making the method more general and scalable in higher dimension with ancillary quantum resource in $\log_2(d)$ qubits order. We realize the universal single-qubit channel corresponding to four Kraus operators [34] simultaneously and can obtain the density information of work qubit under any single Kraus operator. The algorithm is performed in IBM's quantum cloud computer, and the behaviour of entanglement fidelity, entropy and coherent information of different qubit quantum channels which play fundamental role in characterizing the channel capacity are explored. We numerically calculate the capacity of all qubit channels and analyse the behaviour of three important types quantum channels capacity which are general noises affecting the quantum system. The calculation gives a metric on how reliable and efficient of a quantum system to process information undergoes a special channel.

II. QUANTUM ALGORITHM TO REALISE UNIVERSAL QUANTUM CHANNEL

Mathematically, a completely positive and trace preserving linear map is a quantum channel, denoted as the set $\mathfrak{P}(S \mapsto S')$, connecting system S to system S' . In particular, if there exist unitary channels $\mathcal{U}^A \in \mathfrak{P}(S \mapsto S)$ and $\mathcal{U}^B \in \mathfrak{P}(S' \mapsto S')$ satisfy

$$\Phi = \mathcal{U}^B \circ \Lambda \circ \mathcal{U}^A, \quad (2)$$

two maps $\Phi, \Lambda \in \mathfrak{P}(S \mapsto S')$ are unitarily equivalent[38].

A CPTP map expression is also equivalent to operator sum (or Kraus) representation[25, 35, 36],

$$\Phi(\rho) = \sum_{j=1}^r K_j \rho K_j^\dagger. \quad (3)$$

where $\{K_j\}$ are Kraus operators on \mathcal{H}_s which is the Hilbert space of open system and satisfy the completeness conditions $\sum_j K_j^\dagger K_j = I$. The Kraus rank $r = \text{rank}(\tau) \leq d^2$ (d is the dimension of \mathcal{H}_s) is the number of non-zero Kraus operators guaranteeing that a Kraus representation exists with no more than d^2 elements. In the case of single qubit channel, we need at most four Kraus operators to construct a Kraus representation. Specifically, by defining the operator K_j as ${}_E\langle j|U|0\rangle_E$ of \mathcal{H}_S , with $\{|j\rangle_E\}$ is an orthonormal basis of environment E , Kraus representations and the Stinespring dilation are mutual correspondence[38].

Qubit channels are CPTP transformations $\Phi \in \mathfrak{P}(S \mapsto S)$ that map the initial states into final states in the same two dimensional quantum system, denoted $\Phi : \mathcal{M}_2 \rightarrow \mathcal{M}_2$. A linear map Φ on \mathcal{M}_2 can also be represented by

a unique 4×4 matrix \mathbf{T} with 12 independent parameters, which is easy to characterize qubit channels[34].

$$\mathbf{T} = \begin{pmatrix} 1 & \mathbf{0} \\ \mathbf{t} & \mathbf{T} \end{pmatrix} \quad (4)$$

where \mathbf{T} is a 3×3 matrix, \mathbf{t} is column vector and satisfy \mathbf{T} is real. Corresponding to the Bloch ball representation which is more geometrical, this map transforms the state ball into an ellipsoid expressed as

$$\Phi\left(\frac{1}{2}I + \frac{1}{2}\mathbf{r} \cdot \mathbf{s}\right) = \frac{1}{2}I + \frac{1}{2}(\mathbf{t} + \mathbf{r}) \cdot \mathbf{s} \quad (5)$$

where $\mathbf{s} = (\sigma_x, \sigma_y, \sigma_z)^\top$ is a column vector and $\mathbf{r} = (r_x, r_y, r_z) \in \mathbb{R}^3$ of length $|\mathbf{r}| \leq 1$.

For any CPTP map, there always exists an equivalent relationship between two maps. It is $\Phi(\rho) = \mathcal{U}^B [\Phi_\Lambda] \mathcal{U}^A$, where Φ_Λ is a diagonal form via the singular-value decomposition[57]. Φ_Λ is in the closure of the extreme points corresponding to a 4×4 parameterization matrix \mathbf{T} satisfying

$$\mathbf{T} = \begin{pmatrix} 1 & 0 & 0 & 0 \\ 0 & \cos u & 0 & 0 \\ 0 & 0 & \cos v & 0 \\ \sin u \sin v & 0 & 0 & \cos u \cos v \end{pmatrix} \quad (6)$$

where $u \in [0, 2\pi)$ and $v \in [0, 2\pi)$. It is straightforward to prove that this trigonometric parameterization map Φ_Λ can be obtained by the Kraus operators

$$K_0 = \begin{pmatrix} \cos \beta & 0 \\ 0 & \cos \alpha \end{pmatrix}, \quad K_1 = \begin{pmatrix} 0 & \sin \alpha \\ \sin \beta & 0 \end{pmatrix}, \quad (7)$$

where $\alpha = (\mu + \nu)/2$ and $\beta = (\mu - \nu)/2$. According to the theorem in [34], any stochastic map on \mathcal{M}_2 can be written as a convex combination of two maps Φ_Λ in the closure of the extreme points. Namely, an arbitrary single-qubit channel can be realized via four Kraus operators

$$\begin{aligned} K_0 &= \sqrt{P} \begin{pmatrix} \cos \beta_1 & 0 \\ 0 & \cos \alpha_1 \end{pmatrix} \\ K_1 &= \sqrt{P} \begin{pmatrix} 0 & \sin \alpha_1 \\ \sin \beta_1 & 0 \end{pmatrix} \\ K_2 &= \sqrt{1-P} \begin{pmatrix} \cos \beta_2 & 0 \\ 0 & \cos \alpha_2 \end{pmatrix} \\ K_3 &= \sqrt{1-P} \begin{pmatrix} 0 & \sin \alpha_2 \\ \sin \beta_2 & 0 \end{pmatrix}. \end{aligned} \quad (8)$$

where P is the probability from 0 to 1.

Considering K_j is a bounded linear operator in a finite dimensional Hilbert space which can be decomposed into a sum of unitary operators, such that we adopt the duality quantum computing [40–50] to perform the arbitrary single-qubit channel. In duality quantum computing, the work system with initial state $|\Psi\rangle$ and the

d -dimension ancillary system with initial state $|0\rangle$ are coupled together. The corresponding quantum circuit of the algorithm is further shown in Fig. 1.

In the following, the detailed parameters V, W and the controlled gates $U_i \otimes |i\rangle\langle i| (i = 1, \dots, d-1)$ are determined for efficiently simulating the universal single-qubit quantum channel illustrated in equation (9). To make sure W and V being unitary, the Kraus operators are rewritten as

$$\begin{aligned} K_0 &= \sqrt{P} \left[(\cos \beta_1 + \cos \alpha_1) \frac{I}{2} + (\cos \beta_1 - \cos \alpha_1) \frac{Z}{2} \right] \quad (9) \\ K_1 &= \sqrt{P} \left[(\sin \beta_1 + \sin \alpha_1) \frac{X}{2} + (\sin \beta_1 - \sin \alpha_1) \frac{ZX}{2} \right] \\ K_2 &= \sqrt{1-P} \left[(\cos \beta_2 + \cos \alpha_2) \frac{I}{2} + (\cos \beta_2 - \cos \alpha_2) \frac{Z}{2} \right] \\ K_3 &= \sqrt{1-P} \left[(\sin \beta_2 + \sin \alpha_2) \frac{Z}{2} + (\sin \beta_2 - \sin \alpha_2) \frac{ZX}{2} \right] \end{aligned}$$

where I is identity matrix and Z, X are pauli matrix. We define unitary operators $U_0 = U_2 = I, U_1 = U_3 = Z, U_4 = X$.

The unitary operator V is

$$V = \begin{pmatrix} \sqrt{\frac{P(1+\cos(\beta_1-\alpha_1))}{2}} & N & N & N \\ \sqrt{\frac{P(1-\cos(\beta_1-\alpha_1))}{2}} & N & N & N \\ \sqrt{\frac{(1-P)(1+\cos(\beta_2-\alpha_2))}{2}} & N & N & N \\ \sqrt{\frac{(1-P)(1-\cos(\beta_2-\alpha_2))}{2}} & N & N & N \end{pmatrix} \quad (10)$$

where N can be an arbitrary element that satisfies the condition that the matrix V is unitary. The operator W is a 4×4 sparse matrix $[W_1 \ \mathbf{0}; \ \mathbf{0} \ W_2]$ where $\mathbf{0}$ is a 2×2 all-zero matrix. W_1 and W_2 can be illustrated as

$$\begin{aligned} W_1 &= \begin{pmatrix} \frac{\cos \beta_1 + \cos \alpha_1}{\sqrt{2(1+\cos(\beta_1-\alpha_1))}} & \frac{\cos \beta_1 - \cos \alpha_1}{\sqrt{2(1-\cos(\beta_1-\alpha_1))}} \\ \frac{\sin \beta_1 + \sin \alpha_1}{\sqrt{2(1+\cos(\beta_1-\alpha_1))}} & \frac{\sin \beta_1 - \sin \alpha_1}{\sqrt{2(1-\cos(\beta_1-\alpha_1))}} \end{pmatrix} \\ W_2 &= \begin{pmatrix} \frac{\cos \beta_2 + \cos \alpha_2}{\sqrt{2(1+\cos(\beta_2-\alpha_2))}} & \frac{\cos \beta_2 - \cos \alpha_2}{\sqrt{2(1-\cos(\beta_2-\alpha_2))}} \\ \frac{\sin \beta_2 + \sin \alpha_2}{\sqrt{2(1+\cos(\beta_2-\alpha_2))}} & \frac{\sin \beta_2 - \sin \alpha_2}{\sqrt{2(1-\cos(\beta_2-\alpha_2))}} \end{pmatrix} \end{aligned}$$

K_j can be expressed by duality gate $L_j = \sum_i W_{ji} V_{i0} U_i, j = 0, 1, 2, 3$ and a basis changing operation:

$$\begin{aligned} K_0 &= \left(\sum_i W_{0i} V_{i0} U_i \right) I, & K_1 &= \left(\sum_i W_{1i} V_{i0} U_i \right) X \\ K_2 &= \left(\sum_i W_{2i} V_{i0} U_i \right) I, & K_3 &= \left(\sum_i W_{3i} V_{i0} U_i \right) X. \end{aligned} \quad (11)$$

Measuring the final wave functions when the qudit is in state $|j\rangle$ by placing four detectors. The whole process

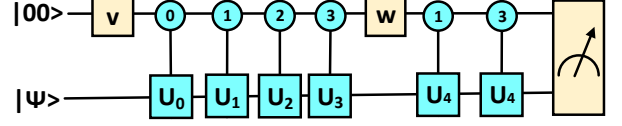


FIG. 1. Quantum circuit to implement the convex combination of two quasiextreme channels. $|\Psi\rangle$ denotes the initial state of principal system, while environment is prepared in the $|00\rangle$ state. V, W are unitary operators to product superposition state and combine the controlled unitary operation respectively. The squares represent unitary operations and the circles represent the state of the controlling qubit. Unitary operations U_0, U_1, U_2 and U_3 are activated only when the auxiliary qubit is $|00\rangle, |01\rangle, |10\rangle$ and $|11\rangle$, respectively. U_4 is active when the auxiliary qubit is $|01\rangle$, or $|11\rangle$.

can be denoted as:

$$\begin{aligned} |00\rangle|\Psi\rangle &\rightarrow E_0|00\rangle|\Psi\rangle + E_1|01\rangle|\Psi\rangle \quad (12) \\ &+ E_2|10\rangle|\Psi\rangle + E_3|11\rangle|\Psi\rangle. \end{aligned}$$

We readout four outputs with the auxiliary system in state $|00\rangle, |01\rangle, |10\rangle$ and $|11\rangle$ respectively and finally realized the four Kraus operators simultaneously. If we only want to obtain the evolution results of the whole quantum channel, measurement on work qubit is enough. Specially, in the condition that the quantum channel corresponding to two Kraus operators or implementing with a classical random number generator [33], only one auxiliary qubit is required to perform the algorithm.

III. EXPERIMENTAL RESULTS FROM THE IBM QUANTUM COMPUTER

A. Realisation of universal qubit channel

Experimentally, we utilize the IBM Quantum Experience project in the cloud, a universal five-qubit quantum computer based on superconducting transmon qubits which has been tested in various ways[51–54], to perform our algorithm and compare the experimental result with the ideal quantum channel. We simplify the quantum circuit with a combination of single qubit gates and controlled NOT gates to carry out the experiment using three superconducting transmon qubits, as shown in Fig. 2. We make a measurement on the work qubit Q_3 to obtain the evolution result after the whole quantum channel. The experimental fidelity is above 98.5% in all the following experiments.

In order to show the feasibility of our algorithm, we totally carried out three classes by changing different parameters in equation (9) and simulate the single qubit quantum channel with the assist of our algorithm for the initial state $\frac{1}{\sqrt{2}}(|0\rangle + |1\rangle)$. For each class, we

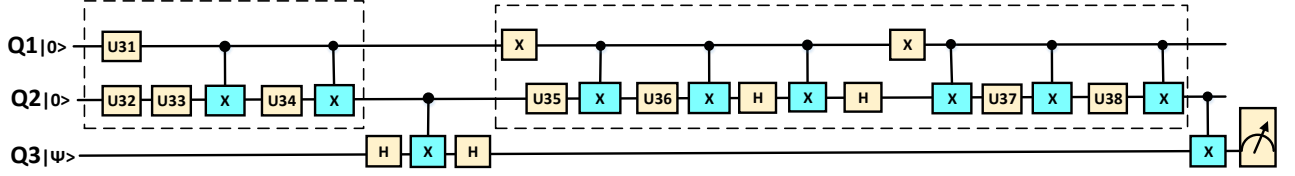


FIG. 2. Digital quantum simulation circuit of the universal quantum channel in IBM cloud. $Q1$ and $Q2$ form the auxiliary system, and $Q3$ is work qubit. The circuit is simplified with only controlled NOT gates required. Further, V and W are decomposed into a combination of single qubit operations and controlled NOT gates as dashed box labeled. This is the final experimental circuit implemented on IBM quantum computer. $U3i$, $i = [1, 2, \dots, 8]$ is unitary rotation operation $R_y(\theta_i)$ depend on the concrete elements of V and W .

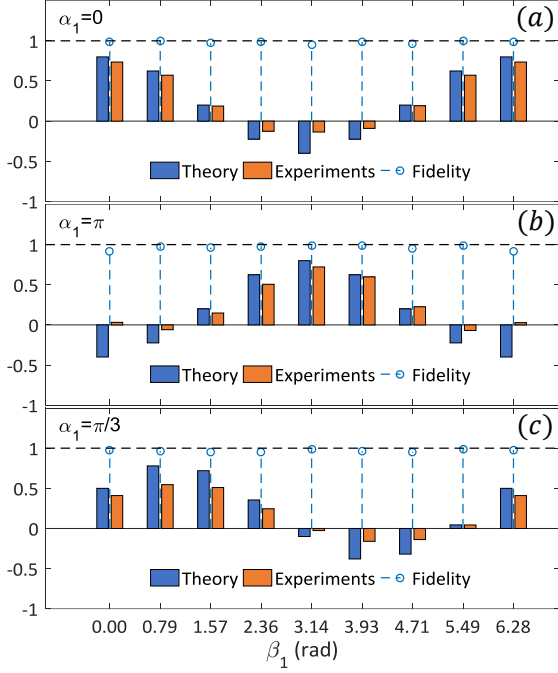


FIG. 3. Experimental results from the IBM quantum computer. The y axes means the expected value $\langle \sigma_x \rangle$ and the fidelity of the final state. In detail, the bars show the comparison between theoretical prediction and experimental results for measuring the expected value $\langle \sigma_x \rangle$. Further, the fidelity between experimental final state ρ_{exp} and theoretical state ρ_{th} is illustrated by the circles.

merely change parameter β_1 from 0 to 2π with the increment $\pi/4$. The detailed setting of the rest parameters: (a) $P = 0.6, \alpha_1 = 0, \alpha_2 = \pi/2$ and $\beta_2 = \pi/6$; (b) $P = 0.6, \alpha_1 = \pi, \alpha_2 = \pi/2$ and $\beta_2 = \pi/6$; (c) $P = 0.6, \alpha_1 = \pi/3, \alpha_2 = \pi/2$ and $\beta_2 = \pi/6$. Each experiment run 8192 shots which means repeating 8192 times to decrease statistical errors. In the end of circuit, the density matrix ρ which reflects the dynamics of the single qubit quantum channel is reconstructed by measuring the expected value of different Pauli operators. Meanwhile, the expected value $\langle \sigma_x \rangle$ and the fidelity of the reconstructed density matrix are presented in Fig. 3. Some properties of single-qubit quantum channel, such

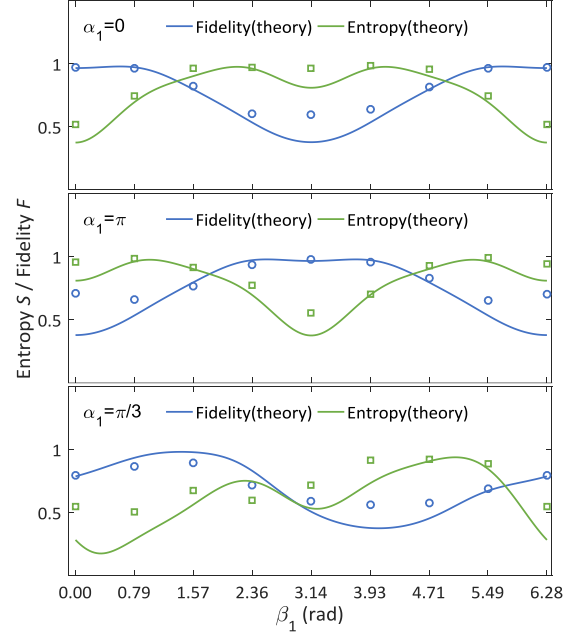


FIG. 4. Experimental results from the IBM quantum computer on the analysis for some properties of quantum channel. In detail, the blue lines illustrate the fidelity between the final state and initial state from theoretical preparation. The cyan lines mean the theoretical von Neumann entropy of the final state. The experimental results are shown by the corresponding square and circle.

as entanglement fidelity and von Neumann entropy, are further analysed by computing the fidelity of the final density matrix with the prepared initial state and the density entropy of final state, whose results are illustrated in Fig. 4. Entanglement fidelity which characterizes how much a system is modified by the action of a channel, is use to study the effectiveness of schemes for sending information through a noisy quantum channel [38, 55]. Entanglement with environment can be characterized using the entanglement entropy,

$$S(\rho_w) = -\text{Tr}(\rho_w \log_2(\rho_w)) \quad (13)$$

where ρ_w is the density matrix of work qubit. The calculation of entropy is critical in determining the channels

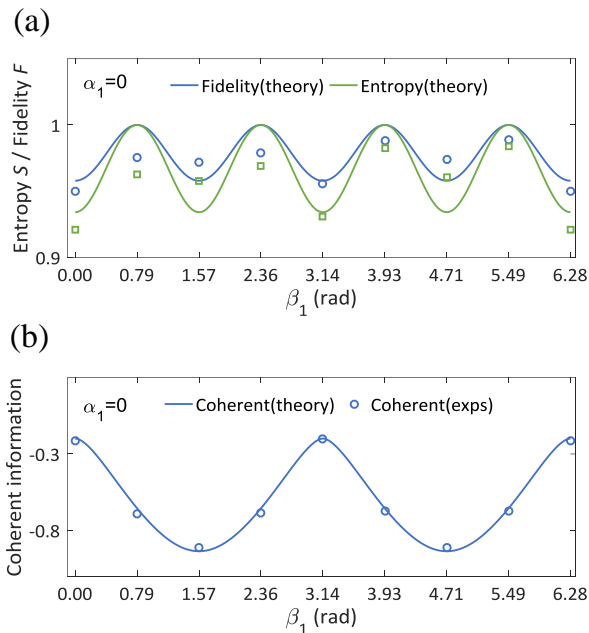


FIG. 5. Behaviors of work qubit with a mixed initial state through quantum channel. (a) The blue lines and the cyan lines show the theoretical fidelity and von Neumann entropy respectively. (b) The channel coherent information is illustrated by the blue lines. Experimental results are shown by the corresponding square and circle with angle β_1 advances from 0 to 2π with the increment $\pi/4$. The rest parameters are fixed as: $P = 0.6$, $\alpha_1 = 0$, $\alpha_2 = \pi/2$ and $\beta_2 = \pi/6$.

efficiency in quantum communication and channels capacity [55].

B. Quantum channel capacity

To discuss the quantum channel more comprehensively, we show the results of quantum channel on a mixed state in Fig .5. We prepare the mixed initial state $\rho_W = \frac{1}{\sqrt{2}}(|0\rangle\langle 0| + |1\rangle\langle 1|)$ which is reduced density operator of a pure state $|\psi\rangle_{WR} = \frac{1}{\sqrt{2}}|00\rangle + \frac{1}{\sqrt{2}}|11\rangle$ of a larger system WR via a purification. In this case, the whole system is consisted of four qubits.

The coherent information roughly measures how much more information work system holds than environment which is analogous to mutual information in classical information theory. It is defined as

$$I(\rho, \Phi) =: S[\Phi(\rho)] - S(\rho; \Phi), \quad (14)$$

where $S(\rho; \Phi) := S[(\Phi \otimes I)(|\psi\rangle_{WR}\langle\psi|)]$. The coherent information of the work system after different quantum channels are given in Fig . 5.

Furthermore, we can calculate the quantum channel capacity by a maximization of the coherent information over all input state [58]

$$C = \text{Max}_\rho I(\rho, \Phi) \quad (15)$$

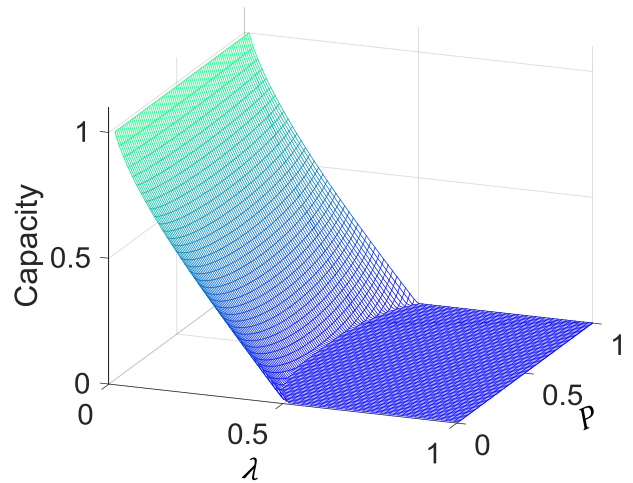


FIG. 6. Quantum capacity of generalized amplitude damping quantum channels. λ and P is the damping rate and temperature of the environment respectively.

The quantum capacity of quantum channels is to quantify the quantum information can be transmitted coherently through a channel and is a critical factor in quantum communications [56]. Thus, we analyse the capacity of some important channels: amplitude damping channel, phase damping channel, and quantum channels corresponding to unital maps.

A generalized amplitude damping (AD) channel describes the effect of dissipation to an environment at finite temperature [25]. The AD channel which is widely inhered in various quantum systems is a critical factor effecting the precision of quantum computation and capacity of quantum communication. For single qubits, it squashes the Bloch sphere towards a given state, denoted as a $\Phi : \mathcal{M}_2 \rightarrow \mathcal{M}_2$ map. Setting $\cos(2\beta_1) = 1$ and $\cos(2\alpha_1) = 1 - 2\lambda$, equation (9) defines the amplitude damping channel with damping rate λ . The damping parameter λ describes the rate of dissipation and parameter P represents the temperature of the environment.

We numerically calculate the capacity of generalized amplitude damping channel with different λ and P . As shown in the picture, with the increasing of dissipation rate in different temperatures of the environment, the quantum capacity is decreased from maximum values to zero. The physical picture is that when the dissipation rate at a finite environmental temperature is large enough, the quantum data can be protected is decreased to zero. It can be used as a standard on measuring the ability of quantum systems that protecting quantum information from the noise environment. The calculation gives a metric on how reliable and efficient of a quantum system to process information undergoes a amplitude damping channel.

A noise channel which describe the loss of quantum information without loss of energy is phase damping (PD) channel[25]. It is quantum mechanical uniquely and is

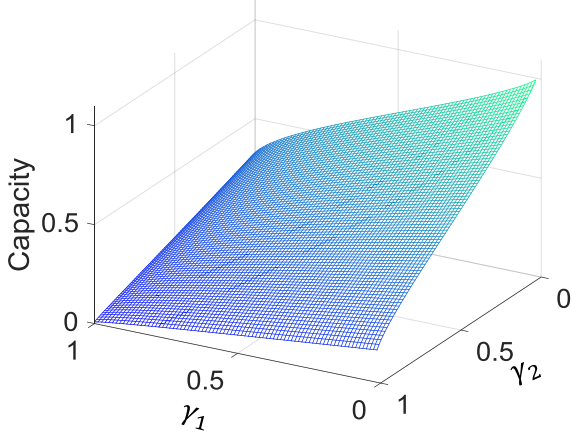


FIG. 7. Behaviours of phase damping quantum channel capacity. γ_1 and γ_2 are the two different strengths of the PD channel.

one of the most subtle process in quantum computation and quantum information, which has drawn an immense amount of study and speculation. It is regarded as a general environment effect leading to our world to be so classical by decreasing and even eliminating coherent information. The phase damping qubit channel squashes the Bloch sphere towards z axis and can be expressed as following

$$K_0 = \sqrt{P} \begin{pmatrix} 1 & 0 \\ 0 & \sqrt{1-\gamma_1} \end{pmatrix}, K_1 = \sqrt{P} \begin{pmatrix} 0 & 0 \\ 0 & \sqrt{\gamma_1} \end{pmatrix}, \quad (16)$$

$$K_2 = \sqrt{1-P} \begin{pmatrix} 1 & 0 \\ 0 & \sqrt{1-\gamma_2} \end{pmatrix}, K_3 = \sqrt{1-P} \begin{pmatrix} 0 & 0 \\ 0 & \sqrt{\gamma_2} \end{pmatrix}.$$

Where the parameter γ_1 and γ_2 can be interpreted as the strength of the PD channel, corresponding to coherence time T_1 and T_2 respectively. It is more general than the PD channel expressed by two Kraus operators which can be obtained in the condition $P = 1$ from Eq. (16). Considering the unitary freedom of quantum operation, the phase damping channel is equal to a recombination of unital channels σ_z and I which can be realised by the universal quantum channel directly. With the coherent strength or coherent time increasing, less and less quantum information can be protected. In the real word, generally, the quantum system mainly undergoing AD and PD channels because of the inevitable coupling with environment. The capacity calculations of AD and PD channels are important to quantify the efficiency to transport quantum information in open quantum system under noise environment.

For $\sin \beta_1 = \pm \sin \alpha_1$ and $\sin \beta_2 = \pm \sin \alpha_2$, one gets unital channels from Eq. (9). Specifically, the depolarizing channel including entanglement breaking (EB) channels is an important type unital channel which transforms the initial state towards the centre of the Bloch sphere.

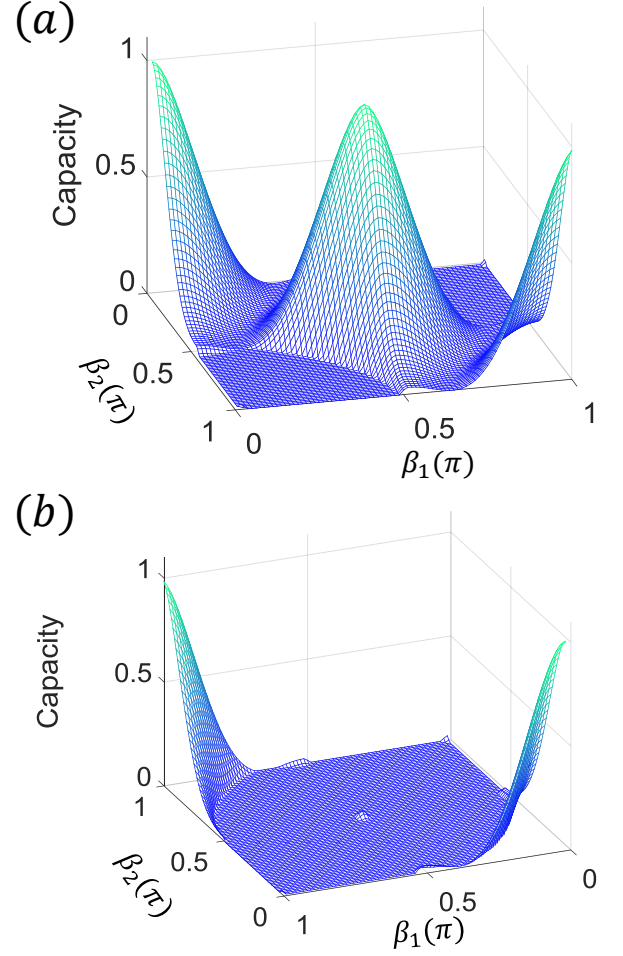


FIG. 8. Capacity of quantum channels corresponding to unital maps. Setting $P = 0.6$, β_1 and β_2 increase from 0 to π by step $\pi/80$.

The capacity of all unital qubit channels is illustrated in Fig. 8. In the case $\sin \beta_1 = \sin \alpha_1$ and $\sin \beta_2 = \sin \alpha_2$, the capacity reaches maximum to 1 when $\beta_1 = \beta_2 = 0, \pi/2, \pi$ as shown in Fig. 8(a). In Fig. 8(b), $\sin \beta_1 = \sin \alpha_1$ and $\sin \beta_2 = -\sin \alpha_2$, there are two maximum values when $\beta_1 = \beta_2 = 0, \pi$.

We experimentally reveal the behaviour of three types of quantum channel capacity: capacity zero channel, amplitude damping channel and capacity maximum channel. In fig. 9(a), a group of Zero-Capacity Channels are shown. With the input state $\frac{1}{\sqrt{2}}(|0\rangle + |1\rangle)$, the coherent information reaches its largest value zero and turn to be the capacity. When it comes to the channel with maximum capacity, we obtain the capacity by calculate the coherent information with maximum mixed state as initial state in fig. 9(b). In fig. 9(c), fixing $P = 0.6$, we show the capacity of amplitude damping channel within the different dissipation rate λ . When $\lambda < 0.4$, the capacity is corresponding to the coherent information with the maximum mixed state as input state. When $\lambda \geq 0.4$,

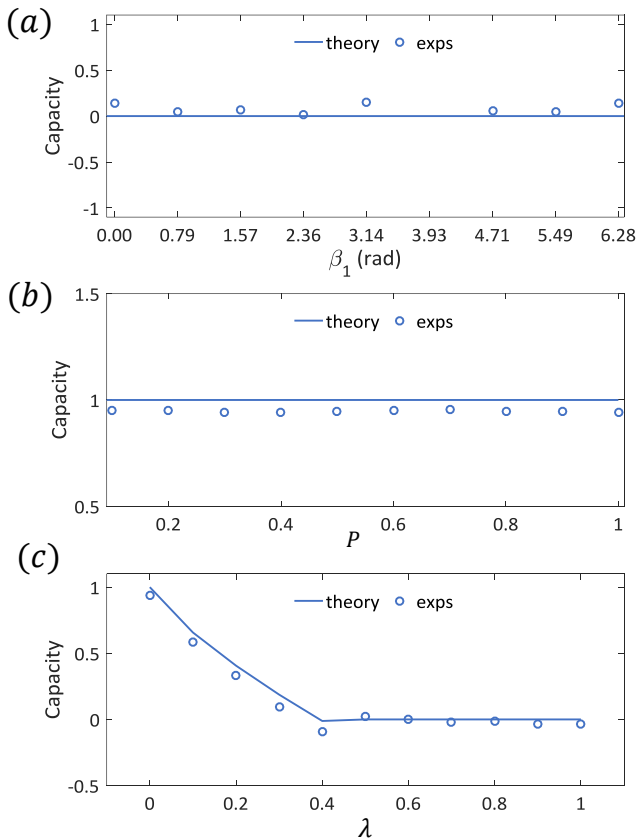


FIG. 9. Three types of quantum channel capacity. (a) Capacity zero channels with parameter β_1 changing from 0 to 2π with the increment $\pi/4$. The rest parameters are fixed as $P = 0.6, \alpha_1 = 0, \alpha_2 = \pi/2$ and $\beta_2 = \pi/6$. (b) Capacity maximum channels with P increasing from 0.1 to 1 by ten steps $\alpha_1 = \beta_1 = \alpha_2 = \beta_2 = \pi/2$. (c) Amplitude damping channels with dissipation rate λ increasing from 0 to 1 with the increment 0.1, $P = 0.6, \beta_1 = \alpha_2 = 0, \alpha_1 = \beta_1 = \arccos(\sqrt{1-\lambda})$. The theoretical capacity is illustrated by the blue lines and experimental results are shown by the corresponding circles.

the capacity is corresponding to the coherent information with the pure state as input state.

Based on the above results, it is believed that the experimental results agree well with the theoretical predictions within a certain errors. Considering that we have repeated the experiment enough times, the statistical errors are reduced. The systematic errors which is mainly contributed by single gate and controlled NOT gates errors is the most important factor leading to the discrepancy with the ideal results.

IV. DISCUSSION

In conclusion, we present a new method to simulate the dynamics of open quantum system by performing the Kraus operators in a linear combination of unitary operators form. We have experimentally shown how to realize

an arbitrary single qubit channel which can be regarded as a primitive for simulating open quantum system dynamics. Our algorithm only requires single direction controlled operation from ancillary system to work qubit and realizes four Kraus operators which correspond to a universal qubit channel simultaneously. Additionally, the ability to obtain the density information of work qubit under any single Kraus operator makes our algorithm flexible and feasible. This method is general and scalable to construct algorithm to simulate the open quantum system dynamics in higher dimension. In our algorithm, the dimension of the ancillary system is determined by the maximum value of number of unitary operators and number of Kraus operators. The maximum value of both are equal to d_s^2 , where d_s is the dimension of the work-qubit system. Consider the fact that any matrix can be written as a linear combination of four unitary matrices [59], the Kraus operator represented quantum channel can be decomposed into a linear combination of four unitary operators in arbitrary dimension. In detail, if the Kraus operators is less than 4, only 2 ancillary qubits are required to perform a quantum channel in any dimension. In the condition that a channel has the number of kraus operators more than 4, we can realize arbitrary dimension quantum channel in the form of convex combination of Kraus operators with the assistance of a number of ancillary qubits that grows logarithmically in the number of Kraus operators. Thus, only in the worst case that the number of Kraus operators is equal to d_s^2 , our method require the same ancillary resource as the standard dilation of a channel.

In our approach, the efficiency is mainly reflected in the gate complexity. According to Ref. [25, 60, 61], a M -qubit arbitrary unitary operation can be implemented using a circuit containing $O(M^3 4^M)$ single qubits and controlled NOT gates. Now, considering a n -qubit original system with a $2n$ -qubit environment, the gate complexity of standard Stinespring dilation method is $O(27n^3 4^{3n})$. In our method, the unitary operations V and W performed on the ancillary system can be decomposed into $O(8n^3 4^{2n})$ single qubits and controlled NOT gates. The controlled operations between V and W can be decomposed into $n 4^{2n}$ single qubit gates and 4^{2n} CNOT gates. Therefore, the total gate complexity of our method is $O(8n^3 4^{2n} + n 4^{2n} + 4^{2n})$. For the large system, it is clearly showed that the improvement of performance is significant compared with Stinespring dilation.

Furthermore, we explore the universal qubit quantum channel properties and calculate the quantum capacity of different channels. The analysis of amplitude damping, phase damping, unital maps channels capacity provides a potential application in quantum communication and information.

The authors would like to thank Bei Zeng for helpful discussions. This work was supported by the National Basic Research Program of China (2015CB921002), the National Natural Science Foundation of China Grant Nos. (11175094, 91221205). Wei is supported by the

-
- [1] R. P. Feynman, *Int. J. Theor. Phys.* **21**, 467 (1982).
- [2] S. Lloyd, *Science*. **273**, 1073 (1996).
- [3] L. Balents, *Nature(London)*. **464**, 199 (2010).
- [4] S. Sachdev, *Quantum Phase Transitions* (Cambridge University Press, Cambridge, England, 1999).
- [5] P. B. Lanyon, J. D. Whitfield, G. G. Gillett, M. E. Goggin, M. Almeida, P. I. Kassal, J. D. Biamonte, M. Mohseni, B. J. Powell, M. Barbieri, A. Aspuru-Guzik, and A. G. White, *Towards quantum chemistry on a quantum computer*, *Nat. Chem.* **2**, 106 (2010).
- [6] J. I. Cirac, P. Maraner, and J. K. Pachos, *Phys. Rev. Lett.* **105**, 190403 (2010).
- [7] A. Bermudez, L. Mazza, M. Rizzi, N. Goldman, M. Lewenstein, and M. A. Martin-Delgado, *Phys. Rev. Lett.* **105**, 190404 (2010).
- [8] R. Gerritsma, G. Kirchmair, F. Zhringer, E. Solano, R. Blatt, and C. F. Roost, *Nature*, **463**, 68-71 (2010).
- [9] D. Bacon, A. M. Childs, I. L. Chuang, J. Kempe, D. Leung, and X. Zhou, *Phys. Rev. A* **64**, 062302 (2001).
- [10] S. Lloyd and L. Viola, *Phys. Rev. A* **65**, 010101(R) (2001).
- [11] H. Weimer, M. Mller, I. Lesanovsky, P. Zoller, and H.-P. Buhler, *Nat. Phys.* **6**, 382 (2010).
- [12] H. Wang, S. Ashhab, and F. Nori, *Phys. Rev. A* **83**, 062317 (2011).
- [13] M. Kliesch, T. Barthel, C. Gogolin, M. Kastoryano, and J. Eisert, *Phys. Rev. Lett.* **107**, 120501 (2011).
- [14] T. Barthel and M. Kliesch, *Phys. Rev. Lett.* **108**, 230504 (2012).
- [15] A. Aspuru-Guzik, A. D. Dutoi, P. J. Love, and M. Head-Gordon, *Science* **309**, 1704 (2005).
- [16] B. M. Terhal and D. P. DiVincenzo, *Phys. Rev. A* **61**, 022301 (2000).
- [17] D. Poulin and P. Wocjan, *Phys. Rev. Lett.* **103**, 220502 (2009).
- [18] M. Mller, S. Diehl, G. Pupillo, and P. Zoller, *Adv. At. Mol. Opt. Phys.* **61**, 1 (2012).
- [19] J. T. Barreiro, M. Mller, P. Schindler, D. Nigg, T. Monz, M. Chwalla, M. Hennrich, C. F. Roos, P. Zoller and R. Blatt *Nature*. **470**, 486 (2011).
- [20] K. L. Brown, W. J. Munro, and V. M. Kendon, *Entropy* **12**, 2268 (2010).
- [21] I. M. Georgescu, S. Ashhab, and F. Nori, *Rev. Mod. Phys.* **86**, 153 (2014).
- [22] T. Prosen and E. Ilievski, *Phys. Rev. Lett.* **107**, 060403 (2011).
- [23] F. Verstraete, M. M. Wolf, and J. I. Cirac, *Nat. Phys.* **5**, 633 (2009).
- [24] W. F. Stinespring, *Proc. Am. Math. Soc.* **6**, 211 (1955).
- [25] Nielsen, M.A. & Chuang I.L. *Quantum Computation and Quantum Information* (Cambridge University Press, 2000).
- [26] M. Mottonen and J. J. Vartiainen, *Trends in Quantum Computing Research* (Nova, New York, 2006), Chap. 7.
- [27] M. P. Almeida, F. de Melo, M. Hor-Meyll, A. Salles, S. P. Walborn, P. H. S. Ribeiro, and L. Davidovich, *Science* **316**, 579 (2007).
- [28] L. Qing, L. Jian, and G. Guang-Can, *Chin. Phys. Lett.* **24**, 1809 (2007).
- [29] T. Hannemann, C. Wunderlich, M. Plesch, M. Ziman, and V. Buzek, arXiv:0904.0923.
- [30] J.-C. Lee, Y.-C. Jeong, Y.-S. Kim, and Y.-H. Kim, *Opt. Express* **19**, 16 309 (2011).
- [31] K. A. G. Fisher, R. Prevedel, R. Kaltenbaek, and K. J. Resch, *New J. Phys.* **14**, 033016 (2012).
- [32] M. Piani, D. Pitkanen, R. Kaltenbaek, and N. Lutkenhaus, *Phys. Rev. A* **84**, 032304 (2011).
- [33] D. S. Wang, D. W. Berry, M. C. de Oliveira, and B. C. Sanders, *Phys. Rev. Lett.* **111**, 130504 (2013).
- [34] M. B. Ruskai, S. Szarek, and E. Werner, *Linear Algebra Appl.* **347**, 159 (2002).
- [35] A. Jamiokowski, *Rep. Math. Phys.* **3**, 275-278 (1972).
- [36] M. D. Choi, *Linear Algebra Appl.* **10**, 285-290 (1975).
- [37] C. King and M. Ruskai, *IEEE Trans. Inf. Theory* **47**, 192 (2001).
- [38] F. Caruso, V. Giovannetti, C. Lupo, and S. Mancini, *Rev. Mod. Phys.* **86**, 1203 (2014).
- [39] A. Jamiokowski, *Rep. Math. Phys.* **3**, 275 (1972); M.-D. Choi, *Linear Algebra Appl.* **10**, 285 (1975).
- [40] G. L. Long, *Commun. Theor. Phys.* **45**, 825-844 (2006).
- [41] G. L. Long, *Int. J. Theor. Phys.* **50**, 1305-1318 (2011).
- [42] G. L. Long, Y. Liu, *Theor. Phys.* **50**, 1303-1306 (2008).
- [43] G. L. Long, Y. Liu, C. Wang, *Commun. Theor. Phys.* **51**, 65-67 (2009).
- [44] S. Gudder, *Quantum Inf. Process.* **6**, 37-48 (2007).
- [45] G. L. Long, *Quantum Inf. Process.* **6**(1), 49-54 (2007).
- [46] S. Gudder, *Int. J. Theor. Phys.* **47**, 268-279 (2008).
- [47] Y. Q. Wang, H. K. Du, Y. N. Dou, *Int. J. Theor. Phys.* **47**, 2268-2278 (2008).
- [48] H. K. Du, Y. Q. Wang, J. L. Xu, *J. Math. Phys.* **49**, 013507 (2008).
- [49] Sh. J. Wei, G. L. Long, *Quantum Inf. Process.* **3**, 1189-1212 (2016).
- [50] Sh. J. Wei, D. Ruan, G. L. Long, *Sci. Rep.* **6**, 30727 (2016).
- [51] IBM Quantum Experience, <http://www.research.ibm.com/quantum>.
- [52] D. Alsina and J. I. Latorre, *Phys. Rev. A* **94**, 012314 (2016).
- [53] S.J. Devitt, *Phys. Rev. A* **94**, 032329 (2016).
- [54] M. Hebenstreit, D. Alsina, J. I. Latorre, B. Kraus, arXiv:1701.02970.
- [55] H. Barnum, M. A. Nielsen, and B. Schumacher, *Phys. Rev. A* **57**, 4153 (1998).
- [56] G. Smith, J. Yard, *Science*, **321**, 5897 (2008).
- [57] C. King, M. Ruskai, *IEEE Trans. Inf. Theory* **47**, 192-209 (2001).
- [58] S. Lloyd, *Phys. Rev. A* **55**, 1613 (1997).
- [59] see the supplemental material for the detail.
- [60] A. Barenco et al., *Phys. Rev. A* **52**, 3457 (1995).
- [61] M. Mttnen, J. J. Vartiainen, V. Bergholm, and M. M. Salomaa, *Phys. Rev. Lett.* **93**, 130502 (2004).

**SUPPLEMENTAL MATERIAL FOR
“EFFICIENT UNIVERSAL QUANTUM CHANNEL SIMULATION IN IBM’S CLOUD QUANTUM
COMPUTER”**

In this supplemental material, we provide some theoretical and experimental details of the employed setup and techniques.

THE THEORY OF IMPLEMENTING NON-UNITARY OPERATORS

The whole process of realising non-unitary operator is shown as following: First, performing the unitary operator V on the auxiliary system to construct a superposition state. Secondly, we implement the auxiliary system controlled operations $U_0 \otimes |0\rangle\langle 0|, U_1 \otimes |1\rangle\langle 1|, \dots, U_{d-1} \otimes |d-1\rangle\langle d-1|$ on the work system. Then, performing the unitary operation W on the auxiliary system. Usually, at this stage, we have realized all the transformations in duality quantum computing. Finally, we readout the results by observing in the subspace of ancillary system. There are at most d outputs in one process by measuring all the eigenvalue states of the ancillary system.

The whole process can be expressed as

$$\begin{aligned}
 |\Psi\rangle|0\rangle &\rightarrow \sum_{i=0}^{d-1} V_{i0}|\Psi\rangle|i\rangle \\
 &\rightarrow \sum_{i=0}^{d-1} V_{i0}U_i|\Psi\rangle|i\rangle \\
 &\rightarrow \sum_i V_{i0}U_i|\Psi\rangle W|i\rangle \\
 &= \sum_i \sum_j W_{ji}V_{i0}U_i|\Psi\rangle|j\rangle \\
 &= \sum_j L_j|\Psi\rangle|j\rangle,
 \end{aligned}$$

where $L_j = \sum_i W_{ji}V_{i0}U_i$ is denoted as the duality quantum gate and $W_{ji}V_{i0}$ is the complex coefficient which satisfies $\sum_{i=0}^{d-1} |W_{ji}V_{i0}| \leq 1$. The duality quantum gate composed by a linear combination of unitary operations is the key to realize Kraus operator.

MATRIX DECOMPOSITION

Any matrix can be written as a linear combination of four unitary matrices. The proof is given as following. Define A as a normalize complex matrix satisfying $\|A\| \leq 1$. Then

$$A = B + iC$$

where B and C are selfadjoint and given by

$$B = \frac{1}{2}(A + A^\dagger), C = \frac{1}{2i}(A - A^\dagger).$$

The two selfadjoint operators satisfy $\|B\| \leq 1$ and $\|C\| \leq 1$, which means that their eigenvalues in the range $[-1, 1]$. Then, B and C can be decomposed as

$$B = \frac{1}{2}(U_1 + U_2), C = \frac{1}{2}(U_3 + U_4).$$

where U_1, U_2, U_3, U_4 are unitary and given by

$$\begin{aligned}
 U_1 &= B + i\sqrt{I - B^2}, U_2 = B - i\sqrt{I - B^2} \\
 U_3 &= C + i\sqrt{I - C^2}, U_4 = C - i\sqrt{I - C^2},
 \end{aligned}$$

Then $A = \frac{1}{2}(U_1 + U_2) + \frac{i}{2}(U_3 + U_4)$ is a linear combination of four unitary matrices.

CHIP ARCHITECTURE AND MEASUREMENT SETUP

The present experiment is performed using three and four superconducting transmon qubits in IBM quantum computer. The superconducting circuits are transmon qubits with resonance frequencies between 5.06 and 5.3 GHz connected by Josephson junctions and shunt capacitors that provide superpositions of charge states. The connections among individual qubits and the classical control system are realised by waveguide resonators. The operations and measurement are achieved by applying tailored microwave signals to this system and measuring the response. Qubits are resolved in the frequency domain during addressing and readout. In the Quantum Experience hardware, it provides four two-qubit interactions. Only the qubits which have interactions, The CNOT gates are allowable. Single-qubit readout fidelities are about $\sim 96\%$ and typical gate fidelities are 99.7% and 96.5% for single qubit gate and the CNOT gates respectively. The pulse time to perform typical single gates and CNOT gates are 130 ns and 250 – 450 ns respectively. The coherence times of two channels both amplitude damping (T_1) and spin dephasing (T_2) are shown as following.

Item	Q1	Q2	Q3	Q4	Q5
$T_1(\mu s)$	58.2	68.1	44.4	48.3	54.1
$T_2(\mu s)$	52.6	40.7	71.7	57.5	88.7